

# Persistence of external chloride and DIDS binding after chemical modification of Glu-681 in human band 3

SONYA BAHAR, CHRISTOPHER T. GUNTER, CHERYL WU,  
SCOTT D. KENNEDY, AND PHILIP A. KNAUF

*Program in Biophysics, Department of Biochemistry and Biophysics,  
University of Rochester Medical Center, Rochester New York 14642*

**Bahar, Sonya, Christopher T. Gunter, Cheryl Wu, Scott D. Kennedy, and Philip A. Knauf.** Persistence of external chloride and DIDS binding after chemical modification of Glu-681 in human band 3. *Am. J. Physiol.* 277 (*Cell Physiol.* 46): C791–C799, 1999.—Although its primary function is monovalent anion exchange, the band 3 protein also cotransports divalent anions together with protons at low pH. The putative proton binding site, Glu-681 in human erythrocyte band 3, is conserved throughout the anion exchanger family (AE family). To determine whether or not the monovalent anion binding site is located near Glu-681, we modified this residue with Woodward's reagent K (*N*-ethyl-5-phenylisoxazolium-3'-sulfonate; WRK). Measurements of Cl<sup>-</sup> binding by <sup>35</sup>Cl-NMR show that external Cl<sup>-</sup> binds to band 3 even when Cl<sup>-</sup> transport is inhibited ~95% by WRK modification of Glu-681. This indicates that the external Cl<sup>-</sup> binding site is not located near Glu-681 and thus presumably is distant from the proton binding site. DIDS inhibits Cl<sup>-</sup> binding even when WRK is bound to Glu-681, indicating that the DIDS binding site is also distant from Glu-681. Our data suggest that the DIDS site and probably also the externally facing Cl<sup>-</sup> transport site are located nearer to the external surface of the membrane than Glu-681.

anion exchangers; anion transport; red blood cells; erythrocytes; nuclear magnetic resonance; anion exchanger 1

---

BAND 3, OR AE1, a 101.7-kDa protein found in the erythrocyte membrane, is a member of the AE family of anion exchangers. Under physiological conditions band 3 catalyzes the one-for-one, electroneutral exchange of Cl<sup>-</sup> and bicarbonate. The protein also mediates the exchange of divalent anions such as sulfate, a process that is accelerated at low extracellular pH (4, 10); the transport of sulfate has been shown to be accompanied by the cotransport of a proton (15).

The zwitterionic reagent Woodward's reagent K (*N*-ethyl-5-phenylisoxazolium-3'-sulfonate; WRK) reacts with carboxyl groups; the typical targets of its effects in proteins are aspartate and glutamate. Jennings and Anderson (18) have shown that when intact red blood cells are treated with WRK at 22°C, there is no detectable reaction with aspartate residues in band 3, as detected by labeling the reaction products with NaB<sup>3</sup>H<sub>4</sub>. At this temperature, both the NH<sub>2</sub>-terminal 60-kDa and the COOH-terminal 35-kDa chymotryptic fragments of band 3 are labeled by WRK plus BH<sub>4</sub>, but when the reaction is run near 0°C, almost all the labeling is in the 35-kDa

fragment. The label in this fragment is almost exclusively on Glu-681 (19). This result is surprising, because another glutamate, Glu-658, is probably located much nearer to the external membrane surface than Glu-681 (34). Conversion of the Glu-681 carboxyl group to an alcohol by WRK plus BH<sub>4</sub> inhibits Cl<sup>-</sup>/Cl<sup>-</sup> exchange and accelerates sulfate/sulfate exchange, sulfate influx into Cl<sup>-</sup>-containing cells (17), and sulfate efflux into Cl<sup>-</sup>-containing media (16). This modification of Glu-681 affects both the intracellular and extracellular pH dependence of band 3-mediated sulfate flux, suggesting that Glu-681 can cross the anion permeation barrier in band 3 and that it is the residue that binds protons in proton-sulfate cotransport (17).

Cotransport of protons and sulfate across the permeability barrier is consistent with a model in which the proton and sulfate binding sites are located near each other in a substrate "pocket" within the protein. The observation that external proton binding increases external sulfate binding affinity and vice versa (26) supports such a picture, although a model in which the binding sites are allosterically coupled is also consistent with this evidence. The increase in sulfate transport observed when the carboxyl group on Glu-681 is converted to the corresponding alcohol by treatment with WRK and BH<sub>4</sub> (17) supports the hypothesis that the sulfate binding site is located near Glu-681. Consistent with this idea, modification by WRK and BH<sub>4</sub>, like external proton binding, also increases external sulfate affinity (M. L. Jennings, personal communication). Mutational studies by Sekler et al. (32) and Chernova et al. (3) with mouse band 3 also implicate Glu-699, the murine analog of Glu-681, in the control of sulfate transport.

Sulfate and Cl<sup>-</sup> are mutually competitive inhibitors of each other's transport (8, 27, 31), and sulfate exchange and Cl<sup>-</sup> exchange are inhibited to the same extent by various concentrations of different transport inhibitors (21). This has led to the idea that the monovalent anion binding site is located in a pocket within the band 3 structure near, or perhaps coincident with, the proton and divalent anion binding sites (26). However, other experiments have shown that the inhibitor *N*-(4-azido-2-nitrophenyl)-2-aminoethylsulfonate interacts differently with Cl<sup>-</sup> than with SO<sub>4</sub><sup>2-</sup> (8), suggesting that monovalent and divalent substrates may not necessarily bind to the same site in band 3.

Kinetic experiments with I<sup>-</sup>, a slowly transported monovalent anion substrate, also support a model in which monovalent and divalent anions bind to different sites. Most of the kinetic data for band 3 can be fitted to a lock-carrier ping-pong model. According to this model,

---

The costs of publication of this article were defrayed in part by the payment of page charges. The article must therefore be hereby marked "advertisement" in accordance with 18 U.S.C. Section 1734 solely to indicate this fact.

there are two different conformations of the protein:  $E_o$ , in which the transport site is accessible to external  $Cl^-$ , and  $E_i$ , in which  $Cl^-$  can bind from the inside or from the cytoplasm. Once  $Cl^-$  is bound, the protein can undergo the "transporting" conformational change from  $E_o$  to  $E_i$  or vice versa. Milanick and Gunn (27) determined the dissociation constants ( $K_d$ ) for the binding of an external proton to the outwardly facing transport site, as well as to this transport site when iodide or sulfate is bound. They found that the  $K_d$  for external  $H^+$  binding to the protein in  $E_o$  was  $1 \times 10^{-5}$  M. When sulfate is bound to the protein in  $E_o$ , the external-proton  $K_d$  is reduced to  $1 \times 10^{-6}$  M, consistent with a picture in which sulfate and  $H^+$  are cotransported and the binding of one ion increases the binding affinity of the other (26). The surprising result, however, is that when  $I^-$  is bound to  $E_o$  the external proton  $K_d$  increases to  $1.2 \times 10^{-5}$  M.

Milanick and Gunn point out that this increase in the proton dissociation constant is contrary to what would be expected from simple electrostatic arguments if the monovalent anion and sulfate/proton binding pockets overlapped. If  $I^-$  were bound in the same position as sulfate, the electrostatic interaction predicts that the  $K_d$  for external  $H^+$  with  $I^-$  bound should decrease to  $3.2 \times 10^{-6}$  M. Further supporting the conclusion that the binding sites for monovalent and divalent anions are not identical, the same authors have observed that internal protons can inhibit the translocation of  $Cl^-$  by binding to band 3 when the  $Cl^-$  transport site is in the unloaded, externally facing form ( $E_o$ ). This implies that an internal proton can bind band 3 in its  $E_o$  conformation. However, the complex of an internal  $Cl^-$  bound to band 3 in  $E_o$  is never observed, which suggests that different gating mechanisms regulate proton and monovalent anion binding and that the two ions' binding sites are distinct (27). This conclusion, however, is based on the assumption that the proton that inhibits  $Cl^-$  transport binds to the same site as the proton involved in  $H^+$ - $SO_4^{2-}$  cotransport. In other words, this interpretation assumes a single  $H^+$  binding site. We address the implications of this assumption in more detail below.

In light of these conflicting observations, it is of great interest to obtain structural as well as kinetic information about the proximity of  $Cl^-$  and  $H^+$  binding sites in band 3. However, structural information from two-dimensional crystals of band 3 (35, 36) so far has insufficient resolution to identify putative substrate binding sites. In the present paper, we examine the relation of the Glu-681 residue to the monovalent substrate binding site by studying the effects of a structural modification of band 3, the reaction of WRK with Glu-681, on  $Cl^-$  binding by  $^{35}Cl^-$ -NMR.

## THEORY

*Measurement of  $Cl^-$  binding to the external transport site of band 3 by  $^{35}Cl^-$ -NMR.* The  $^{35}Cl^-$  nucleus has spin 3/2, and thus there are four nuclear spin states, 3/2, 1/2, -1/2, and -3/2. The binding of  $^{35}Cl^-$  to macromolecules such as band 3 can be observed by NMR because the

$Cl^-$  line width is much larger when the anion is bound than when it is free in solution. The observed  $^{35}Cl^-$  spectra are due to a broadening of the spectral line width of free  $Cl^-$  in solution due to exchange of free  $Cl^-$  with  $Cl^-$  in the bound state (2).

The magnitude of the transverse magnetization ( $M_{trans}$ ) of a  $^{35}Cl^-$ -NMR free induction decay (FID) signal from the extracellular volume of a suspension of erythrocytes may be fitted by a biexponential curve

$$M_{trans} = M_0[0.4e^{-t/T_{2s}} + 0.6e^{-t/T_{2f}}] \quad (1)$$

where  $M_0$  is the initial transverse magnetization,  $T_{2s}$  is the transverse magnetization relaxation time constant for the central transition ( $1/2 \leftrightarrow -1/2$ ),  $T_{2f}$  is the transverse magnetization relaxation time constant for the satellite transitions ( $-3/2 \leftrightarrow -1/2$  and  $1/2 \leftrightarrow 3/2$ ), and  $t$  is the time (2, 23-25, 29). If  $Cl^-$  tumbles rapidly and isotropically in all the environments it experiences,  $T_{2s}$  and  $T_{2f}$  are identical, and the FID signal decays monoexponentially.

Liu et al. (25) have found that the binding of  $Cl^-$  to the externally facing anion transport site of band 3, defined as the part of  $Cl^-$  binding to intact red blood cells that is prevented by pretreatment with disulfonic stilbenes (DS) such as 4',4'-dinitrostilbene-2',2'-disulfonate (DNDS) (6, 7), increases the satellite transition relaxation rate ( $1/T_{2f}$ ) but has little or no effect on the central transition relaxation rate ( $1/T_{2s}$ ). The difference in the effects on  $T_{2s}$  and  $T_{2f}$  is caused by slow and restricted dynamics of  $Cl^-$  motion when bound to band 3. In contrast, Liu et al. (25) observed that  $Cl^-$  binding to DS-insensitive sites on band 3 causes approximately equal increases in  $1/T_{2f}$  and  $1/T_{2s}$ . Therefore, the DS-sensitive contribution to  $1/T_{2f}$  provides the most sensitive means for measuring  $Cl^-$  binding to band 3.

The line width of the  $T_{2f}$  component of the  $Cl^-$  signal ( $LW_f$ ) can be calculated as

$$LW_f = 1/(\pi T_{2f}) \quad (2)$$

The line broadening of the  $T_{2f}$  component ( $LB_f$ ) is then

$$LB_f = LW_f(\text{sample}) - LW(\text{control}) \quad (3)$$

where the control is buffered medium, without erythrocytes (24). In the buffered medium without cells,  $Cl^-$  tumbles rapidly and isotropically, so  $LW_f = LW_s$  and the subscript is dropped. It can be shown (7, 23) that DS-sensitive  $LB_f$  is proportional to the fraction of total  $Cl^-$  bound to band 3

$$LB_f = \alpha P_B = \alpha [Cl^-]_B / [Cl^-]_T = \alpha [X] / ([Cl^-] + K_d) \quad (4)$$

where  $\alpha$  is a proportionality constant related to the relaxation rate at the binding site and to the rate of exchange of free and bound  $Cl^-$ ,  $P_B$  is the probability of an individual external  $Cl^-$  being bound to the transport site, and  $[Cl^-]_B$  is the concentration of  $Cl^-$  bound to the transport site.  $[Cl^-]_T$  is the total concentration of free  $Cl^-$  outside the cells and is equal to the  $Cl^-$  concentration in the suspension medium,  $[Cl^-]$ , when  $[Cl^-]_T \gg [Cl^-]_B$ .  $[X]$  is the concentration of binding sites (e.g., the concentration of band 3).

Hence, by measuring the FID signal under various conditions and fitting its magnitude with *Eq. 1*, we may determine the amount of  $\text{Cl}^-$  bound to the external sides of red blood cells. To avoid contributions to the FID signal from intracellular  $\text{Cl}^-$ , whose relaxation time is very short because of interactions with hemoglobin, the start of signal acquisition was delayed for 1–2 ms after the excitation pulse, by which time almost all of the internal  $\text{Cl}^-$  signal has decayed (25).

Another approach to detecting the binding of  $\text{Cl}^-$  to the band 3 transport site is to measure the  $^{35}\text{Cl}^-$  double-quantum-filtered (DQF) NMR signal, which is accomplished by applying a pulse sequence (see MATERIALS AND METHODS) that creates and selectively detects coherences between spin states separated by two energy levels (13). A  $^{35}\text{Cl}^-$  DQF signal will be detected whenever the decay rates of the central and satellite transitions are not equal, which occurs under the conditions of slow or restricted  $\text{Cl}^-$  dynamics discussed above. We have previously shown that the  $^{35}\text{Cl}^-$  DQF signal from red blood cell suspensions disappears in the presence of DNDS (25). Thus DQF spectra provide information about  $\text{Cl}^-$  binding to the exofacial transport site that is uncontaminated by contributions from nonspecific  $\text{Cl}^-$  binding sites. The disadvantage here is that the DQF signal amplitude is not proportional to the fraction of  $\text{Cl}^-$  bound to band 3. In-depth treatments of DQF signals from quadrupolar nuclei can be found elsewhere (5, 13). We do not attempt to interpret the DQF data presented here in a quantitative manner. However, to provide a qualitative picture of features of the DQF signal, we note that if one assumes that only rank 3 interactions contribute to the double-quantum coherence, then an approximation of the dependence of the DQF signal ( $S_{\text{dqf}}$ ) on the creation time  $\tau$  is given by Eliav and Navon (5)

$$S_{\text{dqf}} \propto [\exp(-\tau/T_{2s}) - \exp(-\tau/T_{2f})](T_{2s} - T_{2f}) \quad (5)$$

This assumes that rank 2 interactions are not present, an assumption we know to be inaccurate from previous work (25). Nonetheless, this expression demonstrates the nonlinear relation between DQF signals and  $\text{Cl}^-$  binding, which is proportional to  $1/T_{2f}$  and  $1/T_{2s}$ , as discussed above.

## MATERIALS AND METHODS

**Cell preparation.** Fresh blood samples were obtained from apparently healthy human donors, with  $\text{Na}^+$ -heparin as the anticoagulant. Cells were washed twice in an ice-cold solution of PBS (150 mM NaCl, 20 mM  $\text{NaH}_2\text{PO}_4$ , pH 6.0) to remove plasma, white blood cells, and fibrin and then twice in 150 KH medium (in mM: 150 KCl, 20 HEPES, 28 sucrose, 5 glucose; pH 7.04 at room temperature). Cells were brought to a concentration of 50% hematocrit (Hct) in 150 KH medium.

**Measurement of  $^{36}\text{Cl}^-$  efflux.** Cells were loaded with  $^{36}\text{Cl}^-$  by incubation at 25% Hct in 150 KH medium, with a trace amount of  $^{36}\text{Cl}^-$  added (usually to a final concentration of 2.5  $\mu\text{Ci}/\text{ml}$  for 25% Hct cells). Cells were incubated for 10 min at room temperature and then placed on ice.

After incubation, 200- $\mu\text{l}$  portions of the cell suspension were placed in 0.4-ml Eppendorf tubes (Sarstedt) and centrifuged for 30 s at 14,000 rpm. The supernatant was removed,

and the pellet of  $^{36}\text{Cl}^-$ -loaded erythrocytes was injected into 30 ml of flux medium, which was mixed by a magnetic stir bar in a chamber kept at 0°C by circulating chilled water-ethanol around it. Cell samples were then withdrawn from the flux chamber with a 10-ml syringe attached to a reversed Swinnex filter holder (4) and an 18-gauge needle. Red blood cells in the medium were filtered out by a 22-mm-diameter no. 24 glass fiber filter (Schleicher & Schuell, Keene, NH) and a type RA filter with a 1.2- $\mu\text{m}$  pore size (Millipore, Bedford, MA). The time at which each filtered supernatant sample was obtained (time of first appearance of liquid in the syringe) was recorded.

To determine  $\text{cpm}(t)$ , the radioactivity in the supernatant at time  $t$ , 600  $\mu\text{l}$  of the supernatant were counted in 5 ml of Ecoscint A or Ecoscint H (National Diagnostics) in a Tricarb 2100TR liquid scintillation analyzer (Packard, Meriden, CT). Duplicate 600- $\mu\text{l}$  samples of unfiltered cell suspension were taken from the flux chamber to obtain  $\text{cpm}(\text{inf})$ , a measure of the total amount of isotope that would be present in the external medium at infinite time. The  $\text{Cl}^-$  efflux rate constant was obtained by a linear fit to a plot of  $\ln[1 - \text{cpm}(t)/\text{cpm}(\text{inf})]$  vs. time (12).

**WRK treatment.** Red blood cells were treated with WRK in a manner similar to that of Jennings and Al-Rhaiyel (17). Cells were prepared as described above, but after washes with PBS and 150 KH medium the cells were resuspended to 10% Hct in ice-cold 150 KH medium. Solid WRK was added to the cell suspension to give a final concentration of 2 mM (calculated on the basis of the total volume of the cell suspension). The cell suspension was gently but well mixed and incubated on ice for 10 min. Cells were then spun down, washed, and resuspended for loading with the radioisotope.

**$^{35}\text{Cl}^-$ -NMR.** Cells were prepared in the same manner as for radioisotope flux experiments, and 3.5- to 4.0-ml samples of cells at 50% Hct were placed in 7-in. glass NMR sample tubes (Wilma Glass, Buena, NJ). Cells were treated with WRK as described above. For the DIDS-treated NMR samples, DIDS (Molecular Probes, Eugene, OR) was added to a concentration of 100  $\mu\text{M}$  (in the total volume of cell suspension) and cells were incubated at 25% Hct at room temperature (and shielded from light) for 30 min. They were then washed once with 150 KH medium and resuspended to 50% Hct before being placed in the NMR sample tube. The length of time between the addition of cells to the sample tube and NMR measurement of the sample was kept to a minimum to avoid lysis, which can cause artifactual increases in  $\text{LB}_f$ . We also attempted to decrease lysis by minimizing the amount of time the cells were kept at high Hct.

All NMR measurements were performed on a 9.4 T Bruker/GE Omega NMR spectrometer (Bruker Instruments, Fremont, CA). The spectrometer operated at a frequency of 39.2 MHz for  $^{35}\text{Cl}$  and 400 MHz for protons. A 10-mm-diameter broad-band tunable probe was used, and the sample was kept at a constant temperature by a flow of nitrogen gas regulated at 3°C over the sample. The sweep width was 2,000 Hz for buffer samples (i.e., samples not containing erythrocytes) and 4,000 Hz for cell samples; 512 points were collected per scan. Shimming was done on the water proton signal for each sample; the solvent proton line width was  $\sim 3$ –5 Hz for buffer and 11 Hz for red blood cell samples. Typically, 5,000 data acquisitions were averaged, requiring a total time of 740 s. As described in THEORY, the magnitude of the FID signal was fitted to a biexponential function (Eq. 1) by the method of least squares with software provided with the instrument.

**DQF NMR.**  $^{35}\text{Cl}^-$  DQF signals were generated with the following pulse sequence (1, 10):  $0^\circ - \tau/2 - 180^\circ - \tau/2 - 90^\circ - \delta - 90^\circ - \text{Acq}$  where  $\tau$  is the creation time and  $\delta$  is a 2- $\mu\text{s}$  delay to reset

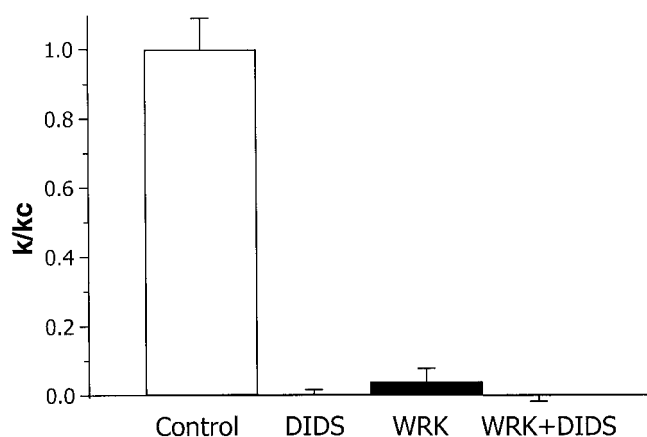


Fig. 1. Woodward's reagent K (WRK) and DIDS effects on  $^{36}\text{Cl}^-$  efflux from erythrocytes. Control cells and cells treated with WRK were loaded with  $^{36}\text{Cl}^-$ , and  $^{36}\text{Cl}^-$  efflux was measured in 150 KH medium at  $0^\circ\text{C}$  as described in MATERIALS AND METHODS. DIDS was added to flux medium at a concentration of  $10\ \mu\text{M}$  where indicated. The  $^{36}\text{Cl}^-$  efflux was inhibited  $99.5 \pm 1.2\%$  (mean  $\pm$  SD;  $n = 5$ ) by DIDS as expected. WRK treatment inhibited transport by  $96 \pm 4\%$  ( $n = 22$ ), and the residual 4% flux was completely eliminated by DIDS (residual flux =  $-0.5 \pm 1.4\%$  of control;  $n = 7$ ). Error bars indicate SD.  $k$ , rate constant for treatment condition;  $k_c$ , rate constant for control cells.

the radio frequency phase. The pulse and receiver phase cycling scheme was that given by Bax et al. (1).

## RESULTS

**Effect of WRK treatment on  $\text{Cl}^-$  transport.** Typical effects of WRK treatment on  $\text{Cl}^-/\text{Cl}^-$  exchange are presented in Fig. 1, which shows the rate constants,  $k$ , for  $\text{Cl}^-$  exchange under various conditions divided by the rate constant for control cells,  $k_c$ . Cells were treated with WRK on ice as described in MATERIALS AND METHODS and then loaded with  $^{36}\text{Cl}^-$ . Efflux took place into 150 KH medium or 150 KH medium with  $10\ \mu\text{M}$  DIDS. The reaction with WRK inhibited  $\text{Cl}^-$  efflux by  $96 \pm 4\%$  (mean  $\pm$  SD), a larger percentage of inhibition than that reported by Jennings (16), who observed 79% inhibition. The higher inhibition may be related to the slightly higher pH in our experiments.

The control flux was inhibited by DIDS to a level (0.5% of control;  $n = 5$ ) that was not significantly different from zero. The flux after WRK treatment was significantly different from zero ( $P < 0.0001$ ,  $n = 22$ ), but it was inhibited to a level ( $-0.5\%$ ;  $n = 7$ ) indistinguishable from zero by DIDS.

**Effect of WRK on external  $\text{Cl}^-$  binding.** To approach the question of the proximity of the external  $\text{Cl}^-$  binding site to Glu-681, we measured  $\text{Cl}^-$  binding to band 3 by  $^{35}\text{Cl}^-$ -NMR in erythrocytes treated with WRK. If the reaction with WRK prevents  $\text{Cl}^-$  binding, this would indicate that the  $\text{Cl}^-$  binding site lies in close proximity to Glu-681 or is affected allosterically by the reaction of WRK with Glu-681. If, however,  $\text{Cl}^-$  binding still takes place in cells that have been treated with WRK, this would mean that the  $\text{Cl}^-$  binding site is not located near Glu-681. Note that this method does not provide us with a means of measuring the precise distance between the  $\text{Cl}^-$  and WRK, so the conclusion

that  $\text{Cl}^-$  is or is not located near Glu-681 must be taken as a qualitative statement. The degree to which any quantitative conclusions can be drawn about the separation between the  $\text{Cl}^-$  binding site and Glu-681 is considered in DISCUSSION.

Figure 2 shows  $\text{LB}_f$  calculated from  $T_{2f}$  obtained from biexponential fits of FID signals in variously treated samples of erythrocytes in  $150\ \text{mM}\ \text{Cl}^-$  medium. As Eq. 4 shows, if  $\alpha$  is constant,  $\text{LB}_f$  is proportional to the fraction of external  $\text{Cl}^-$  bound to the exofacial sides of erythrocytes. In a sample of cells that have not been treated with WRK (Fig. 2, open bar at left), the  $\text{LB}_f$  is  $40.5 \pm 4.0\ \text{Hz}$  (mean  $\pm$  SD;  $n = 5$ ). DIDS treatment causes the  $\text{LB}_f$  to decrease to  $11.2 \pm 2.0\ \text{Hz}$  (Fig. 2, open bar in middle). This indicates that DIDS, a potent DS inhibitor of  $\text{Cl}^-$  transport by band 3, inhibits the binding of  $\text{Cl}^-$  to the exofacial transport site, as do other DS, such as DNDS. Although Falke and Chan (6) reported that, under their conditions, DIDS does not reduce  $\text{Cl}^-$  line broadening as much as does DNDS, Liu (22) has observed identical effects on line broadening by DIDS and DNDS. This may be due to differences in the DIDS treatment conditions.

Cells treated with WRK without the addition of DIDS (Fig. 2) show an  $\text{LB}_f$  of  $27.8 \pm 1.8\ \text{Hz}$ , a value that, although smaller than the  $\text{LB}_f$  for untreated control cells (Fig. 2), is significantly larger than that for the DIDS-treated control sample (Fig. 2). Figure 2 also shows the  $\text{LB}_f$  for a sample of cells treated with both WRK and DIDS. Here  $\text{LB}_f$  is  $11.9 \pm 3.1\ \text{Hz}$ , much lower than that ( $27.8\ \text{Hz}$ ) for WRK-treated cells, indicating that DIDS prevents  $\text{Cl}^-$  binding in WRK-treated cells, just as in control cells (no WRK). This shows that DIDS, a bulky reagent with two negative charges, can still

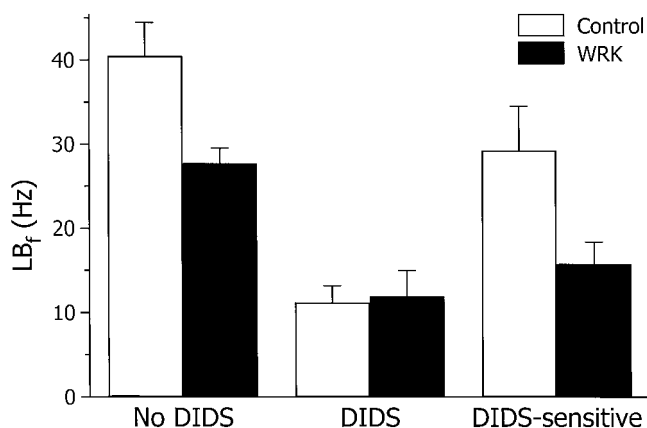


Fig. 2. Effects of WRK and DIDS on  $\text{Cl}^-$  binding to band 3, measured by  $^{35}\text{Cl}^-$ -NMR at  $3^\circ\text{C}$ . Control cells (open bars) and cells treated with WRK (solid bars) were prepared in the same manner as those used for flux measurements shown in Fig. 1. As described in THEORY, line broadening ( $\text{LB}_f$ ) is calculated by subtracting line width (LW) of a  $150\ \text{KH}$  buffer sample from LW of the fast component of free induction decay of a sample of cells at 50% hematocrit suspended in the same buffer. In 1 experiment, which lacked a buffer sample, average of buffer LW ( $19.3 \pm 0.5\ \text{Hz}$ ) for the other experiments was used. No DIDS,  $\text{LB}_f$  from control and WRK-treated cells in absence of DIDS; DIDS, data for cells reacted with  $100\ \mu\text{M}$  DIDS; DIDS-sensitive, difference between  $\text{LB}_f$  with and without DIDS treatment, that is, DIDS-sensitive  $\text{LB}_f$ . Error bars, SD of average values for 5 separate experiments.

gain access to band 3 to block  $\text{Cl}^-$  binding (and hence to inhibit  $\text{Cl}^-$  transport, as seen in Fig. 1) even when WRK has formed a large negatively charged adduct with the  $\text{COO}^-$  group on Glu-681.

Figure 2 shows the DIDS-sensitive  $\text{LB}_f$  for control and WRK-treated cells. The DIDS-sensitive component, which almost certainly represents binding to the exofacial band 3  $\text{Cl}^-$  transport site, is reduced by WRK from  $29.3 \pm 5.3$  to  $15.8 \pm 2.6$  Hz, 54% of its initial value. The  $\text{LB}_f$  remaining after WRK, however, is far larger than that which would be expected on the basis of the unreacted band 3 sites remaining, which would only be  $\sim 4\%$  or 1.2 Hz, as estimated from the transport experiments (Fig. 1). Even if the inhibition were assumed to be as low as 79% (16) only 21% of the DIDS-sensitive  $\text{LB}_f$ , or 6.1 Hz, would remain. The DIDS-sensitive  $\text{LB}_f$  after WRK treatment is significantly different from either of these values, with  $P < 0.01$ . Thus the data indicate that some  $\text{Cl}^-$  is still bound to the external transport site even after band 3 has reacted with WRK.

**Effect of WRK on  $\text{Cl}^-$  affinity.** The decrease in DIDS-sensitive  $\text{LB}_f$  in WRK-treated cells might reflect a decrease in affinity for external  $\text{Cl}^-$  (see Eq. 4). In Fig. 3 we show  $^{35}\text{Cl}^-$   $\text{LB}_f$  measured in WRK-modified cells in media containing different values of external  $\text{Cl}^-$  concentration ( $[\text{Cl}^-]_o$ ) at  $0^\circ\text{C}$ . A fit to these data gives an apparent  $K_d$  value of  $44 \pm 16$  mM for  $\text{Cl}^-$  binding to the external site in WRK-modified band 3. The implica-

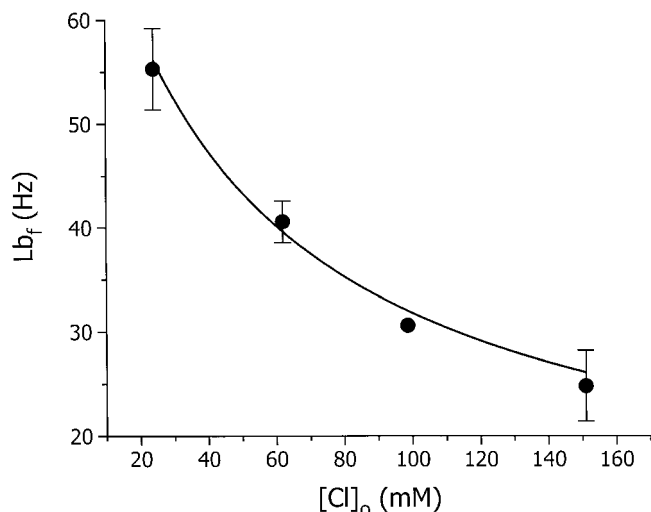


Fig. 3.  $^{35}\text{Cl}^-$ -NMR determination of dissociation constant ( $K_d$ ) for  $\text{Cl}^-$  in WRK-modified band 3 at  $0^\circ\text{C}$ . Cells were washed and treated with WRK in a modified 150 mM  $\text{Cl}^-$  medium (identical to 150 KH, except that it contained 24 mM sucrose and was titrated to pH 6.9 at room temperature) in same manner as in flux experiments shown in Fig. 1;  $\text{LB}_f$  was determined as described in text and in Fig. 2 legend, but at  $0^\circ\text{C}$  instead of at  $3^\circ\text{C}$  and in media with different external  $\text{Cl}^-$  concentrations ( $[\text{Cl}^-]_o$ ), with glutamate replacing  $\text{Cl}^-$ . Data points for 24, 62, 99, and 150 mM  $[\text{Cl}^-]_o$  represent averaged values of 3, 3, 1, and 2 measurements, respectively, compiled from experiments performed on different days but with cells prepared in otherwise identical fashion. Error bars show SD. A nonlinear least-squares fit (solid curve) of data to a modified version of Eq. 4:  $\text{LB}_f = \alpha[\text{X}]/([\text{Cl}^-] + K_d) + \text{LB}_{\text{low}}$ , where  $\text{LB}_{\text{low}}$  is line broadening due to nonspecific (DIDS-insensitive) binding sites and  $[\text{X}]$  is the concentration of binding sites, gives  $K_d = 44 \pm 16$  mM, with  $\text{LB}_{\text{low}}$  fixed at 10 Hz and  $\alpha[\text{X}] = 3,100 \pm 560$  Hz·mM.

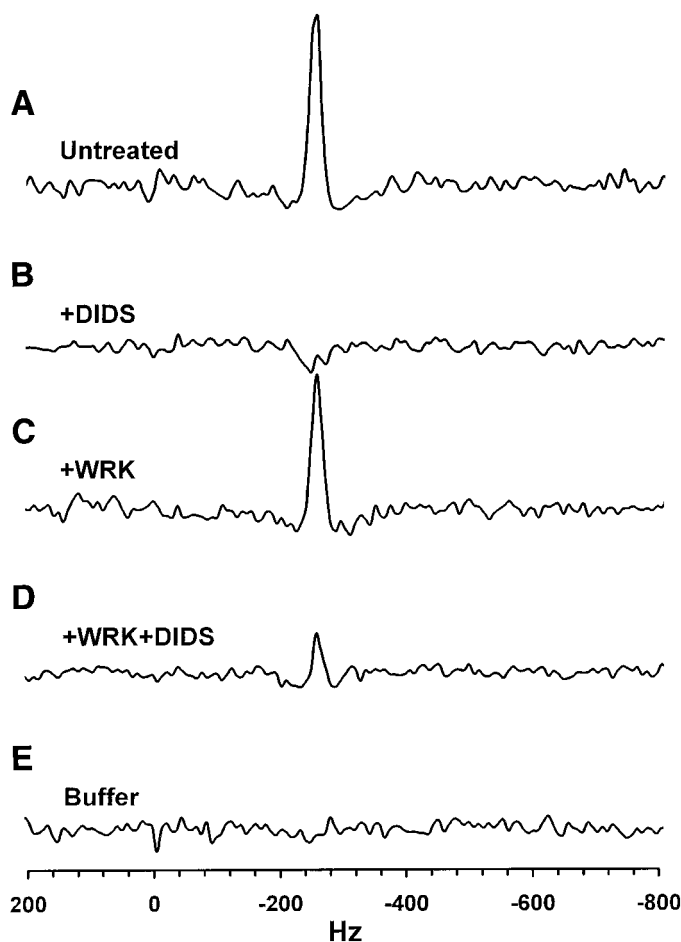


Fig. 4. Double-quantum-filtered (DQF)  $^{35}\text{Cl}^-$ -NMR signals at  $3^\circ\text{C}$ . *A*: control cells. *B*: cells treated with 100  $\mu\text{M}$  DIDS. *C*: cells treated with WRK. *D*: cells treated with WRK and 100  $\mu\text{M}$  DIDS. *E*: buffer (150 KH medium). DQF spectra were acquired as described in MATERIALS AND METHODS with creation time  $\tau = 15$  ms and 2,000 Hz sweep width. For spectra shown in *A* and *C*, 4,800 scans were acquired, and for spectra shown in *B*, *D*, and *E*, 9,600 scans were acquired. Spectra were normalized to same number of scans before display. Each spectrum contains 256 complex data points. Results from 1 data set are shown and are representative of 3 with similar results.

tions of this value in terms of effects of WRK treatment on  $\text{Cl}^-$  affinity are considered in DISCUSSION. It is immediately apparent from Eq. 4, however, that, even if the  $K_d$  value for control cells were negligibly small, the measured  $K_d$  for WRK-treated cells would predict only a 23% decrease in  $\text{LB}_f$  for 150 mM  $[\text{Cl}^-]_o$ ; thus changes in  $K_d$  are not entirely responsible for the decrease in DIDS-sensitive  $\text{LB}_f$  seen in Fig. 2.

**DQF experiments.** We have previously shown that the external  $\text{Cl}^-$  transport site of band 3 is the only external site that substantially restricts the motions of  $\text{Cl}^-$  and that is present in sufficient quantity to give rise to an observable DQF signal (25). Although the DQF signal is not linearly related to the extent of  $\text{Cl}^-$  binding, as is the  $\text{LB}_f$ , it provides a useful qualitative test for band 3-related  $\text{Cl}^-$  binding that is independent of possible problems associated with the double-exponential fitting process that is required to analyze the FID data shown in Fig. 2. Figure 4 shows the DQF

signals from control (A), DIDS-treated (B), and WRK-treated (C) cells, as well as from cells treated with both WRK and DIDS (D). Note that the DQF signal is present in control (untreated) cells, but not in the 150 mM Cl<sup>-</sup> buffer (E) or in DIDS-treated (B) red blood cells. The absence of a DQF signal in DIDS-treated cells demonstrates that the signal arises from a DIDS-protected site(s), presumably the external anion transport site(s).

The DQF signal is only slightly reduced in WRK-treated cells (Fig. 4C) with respect to control (A),<sup>1</sup> and most of this remaining DQF signal can be inhibited by treatment with DIDS (D). This evidence supports the conclusion from Fig. 2 that the binding of Cl<sup>-</sup> to the externally facing transport site and the binding of DIDS to its externally facing binding site are not prevented by the reaction of WRK with Glu-681.

## DISCUSSION

The studies described here reveal a clearer picture of the relation between various binding sites on the band 3 protein. As we have discussed, much previous evidence has been consistent with a simple model in which all band 3 substrates, protons, divalent anions, and monovalent anions, bind to nearby sites in a pocket of the protein possibly close to Glu-681. Our studies, however, support the suggestion of Milanick and Gunn (27) that the relationship between monovalent anion binding sites and the proton binding site is not so simple. Our NMR results are not consistent with a model in which Cl<sup>-</sup> binds near the site of the WRK covalent reaction, and thus presumably are inconsistent with a model in which Cl<sup>-</sup> binds near Glu-681, the putative proton binding site.

*Specificity of WRK for Glu-681.* Jennings and Smith (19) have shown that Glu-681 is the major site of reaction of WRK if the reaction is carried out on ice near neutral pH, but they have also presented evidence that WRK can react with other sites, particularly if the reaction takes place at higher temperature (18) or if red cells are exposed to WRK multiple times (16). Because the present data show the lack of an effect of WRK on Cl<sup>-</sup> and DIDS binding, a reaction at other sites should not affect the conclusion that the WRK reaction at Glu-681 does not affect these processes, so long as there is good evidence that Glu-681 has actually been modified by WRK. Indeed, on the basis of tritiated borohydride cleavage of the WRK reaction products, Jennings and Smith (19) have shown that the reaction on ice labels almost exclusively the 35-kDa COOH-terminal segment of band 3 and that Glu-681 is selectively labeled compared with other glutamate residues in this

segment. However, the reaction at other sites could affect the interpretation of some of the results presented here. For example, if WRK can react with other sites on some band 3 molecules and if this reaction interferes with DIDS binding but does not prevent Cl<sup>-</sup> binding to the external transport site, this would explain why a DIDS-insensitive component of the DQF NMR signal (Fig. 4D) is seen after WRK treatment.

The only way in which a reaction at other sites could affect the main conclusions of this paper would be if some copies of band 3 are modified with WRK only at a site different from Glu-681 and if this modification inhibits Cl<sup>-</sup> exchange without preventing external Cl<sup>-</sup> binding. Such a modification would result in band 3 molecules that cannot transport anions, but whose Glu-681 is intact. The presence of a large population of such band 3 molecules could explain the NMR observations, even if the Glu-681 and Cl<sup>-</sup> binding sites were close together. Because WRK seems to react more avidly with Glu-681 than with other sites (19), this possibility seems highly unlikely.

*Distance between Glu-681 and the Cl<sup>-</sup> binding site.* The reaction of Glu-681 with WRK results initially in the formation of an active ester, which then spontaneously converts to an *N*-acyl derivative (17). Because of conformational flexibility in these adducts, neither completely prevents access to the original glutamate side chain, but either would occupy most of the space within ~5–6 Å of the carboxyl carbonyl group (Fig. 5). Because one end of the adduct formed contains a sulfonic acid group and because the adduct is likely to be formed within a fairly narrow polar “vestibule” within the band 3 protein, it seems unlikely that the Cl<sup>-</sup> binding site could be closer than ~6 Å to Glu-681, and the distance is likely to be considerably longer because of the expected electrostatic repulsion between Cl<sup>-</sup> and the sulfonate moiety of WRK. It is not possible, however, to specify the separation distance precisely from our data, and it should be emphasized that the diagram shown in Fig. 5 is only a schematic representation and is not intended as a precise model for the exact location of WRK within the band 3 vestibule.

*Relation to the work of Milanick and Gunn.* The conclusions of Milanick and Gunn (27) depended in part on the assumption that there is only a single proton binding site and that this site is responsible for both H<sup>+</sup>-SO<sub>4</sub><sup>2-</sup> cotransport and proton inhibition of monovalent anion transport. Working with site-directed mutants of mouse band 3 expressed in *Xenopus* oocytes, however, Müller-Berger et al. (28) found that mutations at Glu-699 (the murine equivalent of Glu-681) and His-752 (equivalent to His-734 in human band 3) have almost identical effects on the external pH dependence of Cl<sup>-</sup> exchange. This raises the possibility that there may be more than one protonatable site in band 3 that affects the pH dependence of anion exchange, thereby shedding doubt on Milanick and Gunn's single-site assumption and the conclusions drawn from it. However, it is possible that His-752 and Glu-699 could act in a cooperative manner to provide a site for proton binding. In such a scenario, the mutation of

<sup>1</sup> Equation 5 predicts a nonlinear relationship between the DQF signal and LB<sub>F</sub>. In particular, at high LB<sub>F</sub> values, such as in control cells, decreases in LB<sub>F</sub> correspond to smaller fractional changes in the DQF signal. For example, for three measurements under the conditions of the DQF experiments in Fig. 4, the LB<sub>F</sub> for WRK-treated cells was an average of 59% of the control LB<sub>F</sub>. The WRK-treated cell/control cell DQF signal ratio predicted from Eq. 5, based on the LB<sub>F</sub> and LB<sub>S</sub> (line broadening of T<sub>2s</sub>) measured from the FID in the same cell samples, was 75 ± 4% (mean ± SD), which was not significantly different (*P* = 0.94) from the measured value of 74 ± 13%.

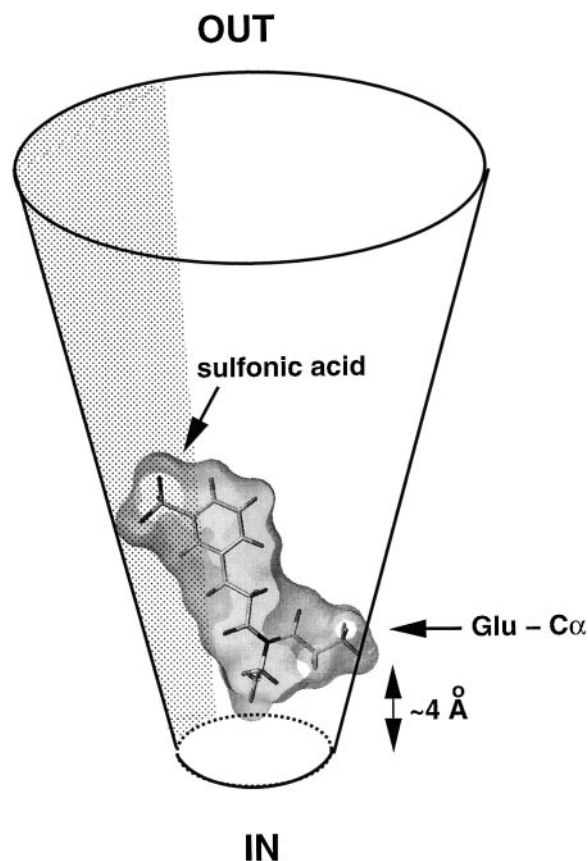


Fig. 5. Schematic representation of the putative hydrophilic access channel in band 3 showing *N*-acyl derivative formed by reaction of WRK with Glu-681. The access channel, through which polar, charged WRK in the external medium presumably gains access to Glu-681, which is located near cytoplasmic side of lipid bilayer (34), is shown as a cone with a height of  $\sim 30$  Å. For clarity, only side chain of Glu-681 is shown; the  $\alpha$ -carbon (Glu- $C\alpha$ ) would be approximately at position indicated by the arrowhead, on the basis of data indicating that Glu-681 is 3rd amino acid from inside of lipid bilayer in an  $\alpha$ -helix (34). A section through the van der Waals surface of the WRK-Glu-681 adduct is shown, together with a stick diagram of the adduct. Note that most of the region near the original Glu-681  $COO^-$  group is occupied by WRK and that sulfonic acid moiety would be expected to extend into the access channel where it should repel other anions such as  $Cl^-$  and DIDS. The *N*-acyl derivative is shown because it is likely that rearrangement to this form occurs during the time interval between WRK treatment and NMR measurements; the initial active ester that is formed would also occlude the region near Glu-681 and would be expected to have sulfonate extending into the access channel. Picture was prepared with Sybyl software courtesy of Dr. B. Goldstein.

either residue might disrupt normal proton binding at a single site, consistent with the postulate of Milanick and Gunn.

In contrast to the kinetic deductions of Milanick and Gunn, the NMR experiments presented here address the relative proximity of Glu-681 and the  $Cl^-$  binding site without requiring any assumptions about other protonatable sites on band 3. Thus the NMR data provide more clear-cut evidence that the Glu-681  $H^+$  binding site is not located near the external  $Cl^-$  transport site.

**Effects of WRK on  $Cl^-$  transport and  $Cl^-$  binding.** Our results indicate that the covalent binding of WRK to Glu-681 does not prevent external  $Cl^-$  binding, al-

though it does prevent  $Cl^-$  transport. The inhibition of anion transport under conditions in which substrate binding is not prevented implies that WRK prevents the translocation event, and thus it must interfere with at least one essential element of the change in band 3 conformation (lock-carrier gating) that causes the change in orientation of the  $Cl^-$  transport site from inside to outside or vice versa. Even if Glu-681 is located at a significant distance from the  $Cl^-$  binding site, the change in band 3 conformation caused by the WRK reaction must affect the gating regions that are likely to be near the transport site, and thus may have a subtle allosteric effect on the environment of  $Cl^-$  bound to the externally facing transport site.

Although the apparent  $K_d$  for external  $Cl^-$  binding in WRK-treated cells ( $44 \pm 16$  mM; Fig. 3) is much higher than the apparent external  $Cl^-$  affinity in untreated cells ( $K_d = 1-3$  mM) on the basis of flux techniques (11), seemingly indicating that WRK decreases the external  $Cl^-$  affinity of band 3, such a comparison is likely to be misleading. The apparent external  $Cl^-$  affinity in untreated cells is a function of several parameters, including  $Cl^-$  affinities at each side of the membrane and the rate constants for the transporting conformational change (25). If, as is likely, WRK prevents the conformational change, it is more reasonable to compare the  $K_d$  value after WRK treatment to that after eosin maleimide (EM) treatment, which also inhibits  $Cl^-$  exchange without preventing external  $Cl^-$  binding (23). Initial experiments gave an external  $Cl^-$   $K_d$  for EM-treated cells of 40–46 mM (24), but more recent measurements by improved data acquisition methods give a somewhat lower value,  $\sim 19$  mM (S. D. Kennedy, C. Wu, and P. A. Knauf, unpublished data). Regardless of which value for EM-treated cells is chosen for comparison, it is apparent that the data in Fig. 3 provide no evidence that WRK causes a major change in external  $Cl^-$  affinity.

In the absence of a major effect on  $K_d$ , the decrease in  $LB_f$  in WRK-treated cells must reflect at least in part an allosteric effect on the factor  $\alpha$  in Eq. 4, which is related to the rate of exchange between external  $Cl^-$  and the binding site, as well as the nature of electric field gradients at the binding site. The reaction of band 3 with EM also causes  $LB_f$  to decrease slightly (23), consistent with a similar decrease in  $\alpha$ , possibly related to changes in protein conformation associated with inhibition of the translocating conformational change.

**Relationship of Glu-681 to the DS binding sites.** We find that the reaction with WRK does not prevent DIDS from inhibiting  $Cl^-$  binding, and hence the DIDS binding site, as well as the  $Cl^-$  binding site, must be some distance from Glu-681. This suggests that Glu-681 is far enough from both the  $Cl^-$  binding site and the DIDS binding site to allow DIDS to inhibit  $Cl^-$  binding even after formation of the WRK-Glu-681 adduct. This conclusion is supported by Jennings and Anderson's observation that reductive methylation affects  $^3H_2$ -DIDS labeling but not WRK- $B^3H_4$  labeling (18) and by Jennings's evidence (M. L. Jennings, personal communication) that reaction of Glu-681 with WRK does not

prevent covalent  $^3\text{H}_2$ -DIDS labeling. On the other hand, Jennings and Anderson (18) have shown that WRK modification of band 3 (measured by  $\text{B}^3\text{H}_4$ -WRK labeling of band 3 or by WRK inhibition of monovalent anion exchange) is greatly inhibited when red blood cells have been treated first with DS such as DNDS or  $\text{H}_2$ -DIDS. This is consistent with a model in which the DS binding site is located closer to the external face of the membrane than Glu-681. Thus DS binding prevents external WRK from reaching Glu-681, but the reaction of WRK with Glu-681 does not prevent DS from gaining access to their binding site.

Although DIDS can bind after WRK treatment, it appears that the binding affinity may be reduced. The DQF results in Fig. 4 suggest that after WRK treatment DIDS is less effective in preventing  $\text{Cl}^-$  binding to band 3. The reason why this is seen in the DQF data (Fig. 4) but not in the  $\text{LB}_f$  (FID) data (Fig. 2) is not clear but may be related to the nonlinear dependence of the DQF signal on  $\text{Cl}^-$  binding to band 3. The conclusion that DIDS affinity is reduced by WRK treatment is supported by data from a single FID experiment (data not shown) in which DIDS treatment was done at  $0^\circ\text{C}$ , at which the covalent reaction is slower (33), and hence differences in reversible binding affinity are more likely to be manifest. Under these conditions, the concentration of DIDS required to give 50% saturation of band 3 binding sites (on the basis of inhibition of  $\text{LB}_f$ ) is  $59 \pm 19 \mu\text{M}$ , over 1,000-fold higher than the corresponding value for untreated cells [31 nM, on the basis of  $\text{Cl}^-$  flux inhibition (14)]. This result should be interpreted cautiously because of the limited data and because the covalent reaction of DIDS continues even at  $0^\circ\text{C}$  during the NMR measurement, making a precise measurement of reversible binding affinity technically impossible, but nevertheless it suggests that there are strong electrostatic, steric, or allosteric interactions between DIDS and WRK.

Although the DIDS and  $\text{Cl}^-$  binding sites share the characteristic of not being blocked by WRK treatment, our results do not necessarily imply that these binding sites overlap. Indeed, Salhany and co-workers (30) have shown that  $\text{Cl}^-$ , band 3, and stilbene disulfonates such as  $\text{H}_2$ -DIDS can form a ternary complex, indicating that stilbene disulfonates and  $\text{Cl}^-$  can both bind to band 3 simultaneously. Although this shows that the stilbene disulfonate site is not identical to the externally facing  $\text{Cl}^-$  transport site, other evidence demonstrates that the binding of DS is very strongly affected by the transport site orientation (9). Thus, even though it is not the transport site, the DS site identifies a part of the band 3 structure that is intimately involved in the transporting conformational change.

*Location of the  $\text{Cl}^-$  binding site and the WRK site relative to the inner surface of the membrane.* The concept that Glu-681 is located nearer to the cytoplasmic surface of the band 3 protein than the DIDS site is consistent with recent cysteine-scanning mutagenesis experiments of Tang et al. (34) with human band 3 expressed in HEK-293 cells. These experiments show that Glu-681 is located in a region of band 3 that is

protected from access to polar reagents, such as biotin maleimide, and that presumably corresponds to a transmembrane  $\alpha$ -helix. Toward the  $\text{NH}_2$  terminus, the nearest residue in this segment that is accessible to biotin maleimide is Met-663, which must be at the external side of the apolar part of the membrane, because the entire region between it and the external *N*-glycosylation site (Asn-642) is accessible to polar reagents. Toward the  $\text{COOH}$ -terminal side of Glu-681, the first accessible residue is Ile-684, indicating that Glu-681 is only three amino acids from the interior side of the apolar portion of the membrane.

The fact that the very polar WRK can reach Glu-681 from the outside implies that there must be an access channel that extends deep into the membrane, allowing external WRK and external protons access to Glu-681. If Glu-681 is the proton transport site, this in turn suggests that protons must only cross a very thin barrier near the inside surface of the membrane to be transported. The same may be true of sulfate, if indeed the sulfate binding site is located near the proton binding site, as suggested if the mutual enhancement of proton and sulfate binding (26) is interpreted on the basis of electrostatic interactions. An important implication of our work is that, because the  $\text{Cl}^-$  binding site is not near Glu-681, it need not be located near the inner membrane surface and could, in fact, be located closer to the external side of the membrane, perhaps near the DIDS site. Even if, as seems likely, there is only a single access vestibule leading into the band 3 protein from the external side, our data imply that the gating structures for  $\text{Cl}^-$  and for protons are located in distinct parts of the protein, probably at different distances from the inside surface of the membrane. Our work, combined with that of Jennings et al. (18, 19), therefore provides biochemical evidence for the separateness of the proton and  $\text{Cl}^-$  gating structures, which is consistent with and which reinforces the kinetic evidence presented by Milanick and Gunn (27). Further work is needed to determine the relationship of the sulfate transport site to these structures.

We gratefully acknowledge Dr. Barry Goldstein's assistance in preparing Fig. 5.

Financial support was provided by National Institute of Diabetes and Digestive and Kidney Diseases Grant DK-27495 and Shared Instrumentation Grant RR-06252.

C.T. Gunter was the recipient of a Strong Children's Research Summer Fellowship.

Portions of this paper have appeared previously in abstract form (20).

Address for reprint requests and other correspondence: S. Bahar, Dept. of Physics, Box 90305, Duke Univ., Durham, NC 27708 (E-mail: bahar@phy.duke.edu).

Received 1 February 1999; accepted in final form 16 June 1999.

## REFERENCES

1. **Bax, A., R. Freeman, and S. P. Kempell.** Natural abundance  $^{13}\text{C}$ - $^{13}\text{C}$  coupling observed via double-quantum coherence. *J. Am. Chem. Soc.* 102: 4849–4851, 1980.
2. **Bull, T. E.** Nuclear magnetic relaxation of spin-3/2 nuclei involved in chemical exchange. *J. Magn. Reson.* 8: 344–353, 1972.
3. **Chernova, M. N., L. Jiang, M. Crest, M. Hand, D. Vandorpe, K. Strange, and S. L. Alper.** Electrostatic sulfate/chloride



- exchange in *Xenopus* oocytes mediated by murine AE1 E699Q. *J. Gen. Physiol.* 109: 345–360, 1997.
4. **Dalmark, M.** The effect of temperature, bicarbonate/CO<sub>2</sub>, and pH on the chloride transport across the human red cell membrane. In: *Oxygen Affinity of Hemoglobin and Red Cell Acid-Base Status*, edited by M. Rørth and P. Astrup. Copenhagen: Munksgaard, 1972, p. 320–326.
  5. **Eliav, U., and G. Navon.** Analysis of double-quantum-filtered NMR spectra of <sup>23</sup>Na in biological tissues. *J. Magn. Reson. B* 103: 19–29, 1994.
  6. **Falke, J. J., and S. I. Chan.** Molecular mechanisms of band 3 inhibitors. I. Transport site inhibitors. *Biochemistry* 25: 7888–7894, 1986.
  7. **Falke, J. J., R. J. Pace, and S. I. Chan.** Chloride binding to the anion transport binding sites of band 3. A <sup>35</sup>Cl NMR study. *J. Biol. Chem.* 259: 6472–6480, 1984.
  8. **Fröhlich, O., and R. B. Gunn.** Interactions of inhibitors on anion transporter of human erythrocyte. *Am. J. Physiol.* 252 (*Cell Physiol.* 21): C153–C162, 1987.
  9. **Furuya, W., T. Tarshis, F.-Y. Law, and P. A. Knauf.** Transmembrane effects of intracellular chloride on the inhibitory potency of extracellular H<sub>2</sub>DIDS. Evidence for two conformations of the transport site of human erythrocyte anion exchange protein. *J. Gen. Physiol.* 83: 657–681, 1984.
  10. **Gunn, R. B.** A titratable-carrier model for both mono- and di-valent anion transport in human red blood cells. In: *Oxygen Affinity of Hemoglobin and Red Cell Acid-Base Status*, edited by M. Rørth and P. Astrup. Copenhagen: Munksgaard, 1972, p. 823–827.
  11. **Gunn, R. B., and O. Fröhlich.** Asymmetry in the mechanism for anion exchange in human red blood cell membranes. Evidence for reciprocating sites that react with one transported anion at a time. *J. Gen. Physiol.* 74: 351–374, 1979.
  12. **Gunn, R. B., and O. Fröhlich.** Methods and analysis of erythrocyte anion fluxes. *Methods Enzymol.* 173: 54–80, 1989.
  13. **Jaccard, G., S. Wimperis, and G. Bodenhausen.** Multiple-quantum NMR spectroscopy of S = 3/2 spins in isotropic phase: a new probe for multiexponential relaxation. *J. Chem. Phys.* 85: 6282–6293, 1986.
  14. **Janas, T., P. J. Bjerrum, J. Brahm, and J. O. Wieth.** Kinetics of reversible DIDS inhibition of chloride self-exchange in human erythrocytes. *Am. J. Physiol.* 257 (*Cell Physiol.* 26): C601–C606, 1989.
  15. **Jennings, M. L.** Proton fluxes associated with erythrocyte membrane anion exchange. *J. Membr. Biol.* 28: 187–205, 1976.
  16. **Jennings, M. L.** Rapid electrogenic sulfate-chloride exchange mediated by chemically modified band 3 in human erythrocytes. *J. Gen. Physiol.* 105: 21–47, 1995.
  17. **Jennings, M. L., and S. Al-Rhaiyel.** Modification of a carboxyl group that appears to cross the permeability barrier in the red blood cell anion transporter. *J. Gen. Physiol.* 92: 161–178, 1988.
  18. **Jennings, M. L., and M. P. Anderson.** Chemical modification and labeling of glutamate residues at the stilbenedisulfonate site of human red blood cell band 3 protein. *J. Biol. Chem.* 262: 1691–1697, 1987.
  19. **Jennings, M. L., and J. S. Smith.** Anion-proton cotransport through the human red blood cell band 3 protein: role of glutamate-681. *J. Biol. Chem.* 267: 13964–13971, 1992.
  20. **Knauf, P. A., S. Bahar, C. T. Gunter, C. Wu, and S. D. Kennedy.** External Cl<sup>-</sup> and DIDS binding to band 3 persist after modification of Glu-681 (Abstract). *FASEB J.* 12: A1032, 1998.
  21. **Ku, C.-P., M. L. Jennings, and H. Passow.** A comparison of the inhibitory potency of reversibly acting inhibitors of anion transport on chloride and sulfate movements across the human red cell membrane. *Biochim. Biophys. Acta* 553: 132–141, 1979.
  22. **Liu, D.** *Study of Cl<sup>-</sup> Binding to the External Facing Transport Site of Band 3 by <sup>35</sup>Cl NMR* (PhD dissertation). Rochester, NY: Univ. of Rochester Medical Center, 1996.
  23. **Liu, D., S. D. Kennedy, and P. A. Knauf.** <sup>35</sup>Cl nuclear magnetic resonance line broadening shows that eosin-5-maleimide does not block the external anion access channel of band 3. *Biophys. J.* 69: 399–408, 1995.
  24. **Liu, D., S. D. Kennedy, and P. A. Knauf.** Source of transport site asymmetry in the band 3 anion exchange protein determined by NMR measurements of external Cl<sup>-</sup> affinity. *Biochemistry* 35: 15228–15235, 1996.
  25. **Liu, D., S. D. Kennedy, and P. A. Knauf.** Detection of Cl<sup>-</sup> binding to band 3 by double-quantum-filtered <sup>35</sup>Cl nuclear magnetic resonance. *Biophys. J.* 70: 715–722, 1996.
  26. **Milanick, M. A., and R. B. Gunn.** Proton-sulfate cotransport: mechanism of hydrogen and sulfate addition to the chloride transporter of human red blood cells. *J. Gen. Physiol.* 79: 87–113, 1982.
  27. **Milanick, M. A., and R. B. Gunn.** Proton inhibition of chloride exchange: asynchrony of band 3 proton and anion transport sites? *Am. J. Physiol.* 250 (*Cell Physiol.* 19): C955–C969, 1986.
  28. **Müller-Berger, S., D. Karbach, D. Kang, N. Aranibar, P. G. Wood, H. Rüterjans, and H. Passow.** Roles of histidine 752 and glutamate 699 in the pH dependence of mouse band 3 protein mediated anion transport. *Biochemistry* 34: 9325–9332, 1995.
  29. **Price, W. S., P. W. Kuchel, and B. A. Cornell.** A <sup>35</sup>Cl and <sup>37</sup>Cl NMR study of chloride binding to the erythrocyte anion transport protein. *Biophys. Chem.* 40: 329–337, 1991.
  30. **Salhany, J. M., R. L. Sloan, K. A. Cordes, and L. M. Schopfer.** Kinetic evidence of ternary complex formation and allosteric interactions in chloride and stilbenedisulfonate binding to band 3. *Biochemistry* 33: 11909–11916, 1994.
  31. **Schnell, K. F., S. Gerhardt, and A. Schoppe-Fredenburg.** Kinetic characteristics of the sulfate self exchange in human red blood cells and red cell ghosts. *J. Membr. Biol.* 30: 319–350, 1977.
  32. **Sekler, I., R. S. Lo, and R. R. Kopito.** A conserved glutamate is responsible for ion selectivity and pH dependence of the mammalian anion exchangers AE1 and AE2. *J. Biol. Chem.* 270: 28751–28758, 1995.
  33. **Ship, S., Y. Shami, W. Breuer, and A. Rothstein.** Synthesis of tritiated 4,4'-diisothiocyano-2,2'-stilbene disulfonic acid ([<sup>3</sup>H]DIDS) and its covalent reaction with sites related to anion transport in human red blood cells. *J. Membr. Biol.* 33: 311–323, 1977.
  34. **Tang, X.-B., J. Fujinaga, R. Kopito, and J. R. Casey.** Topology of the region surrounding Glu<sup>681</sup> of human AE1 protein, the erythrocyte anion exchanger. *J. Biol. Chem.* 273: 22545–22553, 1998.
  35. **Wang, D. N., W. Kuhlbrandt, V. E. Sarabia, and R. A. F. Reithmeier.** Two-dimensional structure of the membrane domain of human band 3, the anion transport protein of the erythrocyte membrane. *EMBO J.* 12: 2233–2239, 1993.
  36. **Wang, D. N., V. E. Sarabia, R. A. F. Reithmeier, and W. Kuhlbrandt.** Three-dimensional map of the dimeric membrane domain of the human erythrocyte anion exchanger band 3. *EMBO J.* 13: 3230–3235, 1994.